Solid State Communications 150 (2010) 36–39

Contents lists available at ScienceDirect

Solid State Communications

journal homepage: www.elsevier.com/locate/ssc

Physical properties of the 5M $BaIrO_3$: A new weak ferromagnetic iridate synthesized under high pressure

J.G. Zhao [a,b], L.X. Yang [a], Y. Yu [a], F.Y. Li [a], R.C. Yu [a], C.Q. Jin [a,*]

[a] *Beijing National Lab for Condensed Matter Physics, Institute of Physics, Chinese Academy of Sciences, Beijing 100190, PR China*

[b] *Natural Science Research Center, Academy of Fundamental and Interdisciplinary Sciences, Harbin Institute of Technology, Harbin 150080, PR China*

ARTICLE INFO

Article history:
Received 2 July 2009
Received in revised form
29 August 2009
Accepted 7 October 2009 by D.D. Sarma
Available online 12 October 2009

PACS:
07.35.+k
71.27.+a
72.80.Ga
72.15.Eb

Keywords:
A. Barium iridate
D. Weak ferromagnetism
D. Electrical property

ABSTRACT

The 5M $BaIrO_3$, which is intervenient in the 9M and 6M forms, was synthesized under high pressure and high temperature, and the physical properties were obtained. The measurement of low-temperature electrical resistivity shows that the 5M $BaIrO_3$is a Fermi-Liquid metal, because of the linear relationship of ρ versus T^2 at low temperature. The relationships of magnetic susceptibility versus temperature indicate that the 5M $BaIrO_3$ is a weak ferromagnet, with the Curie temperature T_c about 54.3 K. According to the Wilson ratio R_W of 1.67(4) and Stoner enhancement factor S of 2.8 calculated through the low-temperature specific heat data, there is a modest electron–electron correlation effect in the 5M $BaIrO_3$.

1. Introduction

In recent years, the oxide iridates have received growing attention for their exotic physical properties. For example, the ambient-pressure phase of $BaIrO_3$ is the first known ferromagnet that contains a 5d transition metal cation in a ternary oxide [1]. The iridate $BaIrO_3$ is very similar with the ruthenate $BaRuO_3$ in the structural and physical properties. There are three types of hexagonal perovskite-type $BaRuO_3$ reported, namely 9R, 4H, and 6H [2–5], where the number is the amount of BaO_3 layers in a unit cell, and the R and H denote the rhombohedral (space group: $R\bar{3}m$) and hexagonal (space group: $P6_3/mmc$) structures, respectively. In one unit cell, the stacking sequence of BaO_3 layers along the c-axis is $(hhc)_3$, $(hc)_2$, $(hcc)_2$ for the 9R, 4H, and 6H $BaRuO_3$, respectively, where the h and c are hexagonal close stacking and cubic close stacking, respectively.

Being different from $BaRuO_3$, $BaIrO_3$ crystallizes into the monoclinic structure. The ambient $BaIrO_3$ adopts the space group $C2/m$, with a stacking sequence $(hhc)_2$ along the c-axis [6]. Its crystal structure is closely related to that of the 9R $BaRuO_3$, so it is denoted as 9M, due to the monoclinic structure. By treating the 9M $BaIrO_3$ at 5 GPa and 1000 °C, we obtained the 6M $BaIrO_3$, with the space group $C2/c$ [7]. The crystal structure of the 6M $BaIrO_3$ is similar with that of the ambient $SrIrO_3$, with a stacking sequence $(hcc)_2$ along the c-axis [8]. We also obtained an uncertain structure of $BaIrO_3$ at 3.3–4.0 GPa and 1000 °C at the same time [7]. Recently, Cheng et al. found that this new form adapts a 5-layer structure, with the space group $C2/m$ [9]. We denoted this new polymorph of $BaIrO_3$ as 5M, which is intervenient in the 9M and 6M forms. Along the c-axis, the stacking sequence is $hchcc$ in the 5M $BaIrO_3$.

The 9M $BaIrO_3$ is a weak ferromagnet, with the Curie temperature T_c about 183 K [1,10]. It is the first known ferromagnet that contains a 5d transition metal cation in a ternary oxide, which originates from spin polarization of Ir cations rather than spin canting [11,12]. The polycrystalline sample is a semiconductor [13], with an obvious kink in the ρ–T curve that corresponds to the Curie temperature T_c. For the single crystal, along the c-axis that is the high conductivity axis, the 9M $BaIrO_3$ transforms to a more insulating phase below T_c, and then transforms to metallic and insulating states at 80 K and 26 K, respectively [11,12]. This metal–insulator transition is ascribed to the charge density wave (CDW) formation in the 9M $BaIrO_3$, where the transition temperature T_{CDW} is equal to about 26 K. Like the 6H $BaRuO_3$, the 6M $BaIrO_3$ is an abnormal metal, being deviated from the Fermi liquid behavior, following a

---

* Corresponding author. Tel.: +86 10 82648041; fax: +86 10 82640223.
E-mail address: zhaojinggeng@163.com (C.Q. Jin).

0038-1098/$ – see front matter © 2009 Elsevier Ltd. All rights reserved.
doi:10.1016/j.ssc.2009.10.012

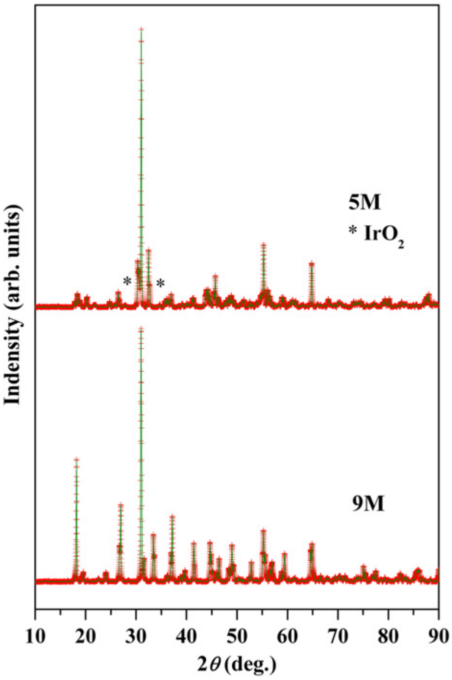

Fig. 1. The x-ray diffraction patterns of the 9M and 5M BaIrO$_3$. The peaks of IrO$_2$ impurity are indexed with the asterisks.

linear relationship of ρ versus T below 20 K [7]. Both magnetic susceptibility and specific heat data indicate that it is an exchange-enhanced Pauli paramagnet, because of the electron–electron correlation effect. Up to now, there are no reports about the physical properties of the 5M form. In this paper, we research the electrical and magnetic properties of the 5M BaIrO$_3$.

2. Experiment

The 9M BaIrO$_3$ was synthesized by using the conventional solid-state chemical reaction [14]. The starting materials were barium carbonate and iridium metal of 99.9% purity. Stoichiometric quantities of materials were mixed together, ground for about 30 min in an agate mortar, and placed into an Al$_2$O$_3$ crucible. Then the powder was calcined for about 12 h at 900 °C in air. The calcined powder was reground, pressed into a pellet at the pressure of 10 MPa, and sintered at 1000 °C for about 72 h in air with two intermediate grindings. The product was polycrystalline powder in black.

A conventional cubic-anvil type high-pressure facility was used to perform the high-pressure and high-temperature experiments. The 9M BaIrO$_3$ material was pressed into a pellet of 5.0 mm diameter, and then wrapped with gold foil to avoid contamination. The pellet was put into an h-BN sleeve which was, in turn, inserted into a graphite tube heater. Pyrophyllite was used as the pressure-transmitting medium. The treating process was carried out at 4 GPa and 1000 °C for about 30 min, followed by a quench from high temperature before pressure release, with the rate about 0.6 GPa/min. The product is the 5M BaIrO$_3$, which is black and hard polycrystal.

The structures of our samples were checked by the powder x-ray diffraction (XRD) with CuK$_\alpha$ radiation at room temperature, using a Rigaku diffractometer (MXP-AHP18). Fig. 1 shows the XRD patterns of the 9M and 5M BaIrO$_3$. There are a few IrO$_2$ in the 5M BaIrO$_3$, indexed with the asterisks in Fig. 1. The existence of IrO$_2$ is due to the partial decomposition of the 9M BaIrO$_3$, because the precursor is pure [14]. IrO$_2$ is a paramagnetic metal, with very small electrical resistivity and magnetic susceptibility in a large temperature range [15,16]. So the effect of IrO$_2$ on the physical properties of the 5M BaIrO$_3$ is very small. In the 5M BaIrO$_3$, there are also a few 9M BaIrO$_3$. The content of the 9M form does not exceed 3% in the whole compound, so it can only produce a little effect on the physical properties of the 5M BaIrO$_3$.

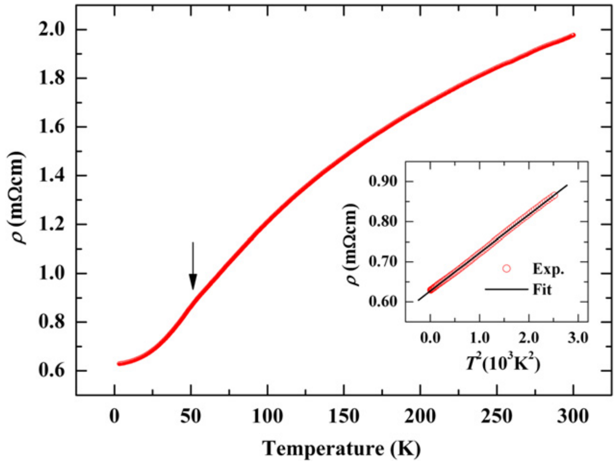

Fig. 2. Temperature dependence of electrical resistivity of the 5M BaIrO$_3$. The inset shows the linear relationship of ρ versus T^2.

The measurement of temperature dependence of electrical resistivity was performed by using the four-probe method with Ag paste contacts on an Oxford Maglab measuring system in the temperature range of 3–300 K. The relationships of magnetic susceptibility versus temperature were obtained using a SQUID magnetometer (Quantum Design, MPMS-5S) in the temperature range of 5–300 K. Data were collected under both zero-field-cooled (ZFC) and field-cooled (FC) conditions, with the magnetic field $H = 0.1$ T. The magnetic field dependences of magnetization were measured from −3 to 3 T at different temperatures. The heat-capacity measurement was carried out using a heat pulse relaxation technique by a commercial heat capacity measuring system (Quantum Design, PPMS equipment) in the temperature range of 2–30 K. The sample was mounted on a thin alumina plate with grease for better thermal contact.

3. Results and discussion

The temperature dependence of electrical resistivity of the 5M BaIrO$_3$ is shown in Fig. 2. The 5M BaIrO$_3$ maintains the metallic behavior down to the lowest temperature in our experiment. The electrical resistivity does not show the linear dependence of temperature above 100 K, as predicated by normal Bloch extended band theory based on phonon scattering mechanism. There is an obvious turning point at about 52 K in the ρ–T curve, which corresponds to the Curie temperature T_c, indicated with an arrow in Fig. 2. The relationship of electrical resistivity versus temperature of the 5M BaIrO$_3$ is similar to that of the cubic BaRuO$_3$ [17,18]. The electrical resistivity below T_c approximately follows the equation $\rho = \rho_0 + AT^2$, which indicates that the 5M BaIrO$_3$ is a normal Fermi-liquid metal. The linear relationship of electrical resistivity versus T^2 is shown in the inset of Fig. 2. Through fitting the ρ–T curve, the ρ_0 of 0.6271(2) mΩ cm and A of 9.50(1) $\times 10^{-5}$ mΩcm/K^2 are obtained. The residual resistivity ratio ($RRR = \rho_{300\ K}/\rho_{T\to 0}$) for the 5M BaIrO$_3$ is approximately equal to 3. The ρ_0 and RRR for the 5M BaIrO$_3$ are approximately equal to those of the 6M BaIrO$_3$ [7]. According to the crystal structure, the metallicity of the 5M BaIrO$_3$ should be better than the 6M form, because the proportion of direct Ir–Ir interaction in the former is larger than that in the latter [9,7]. But, due to the 9M BaIrO$_3$ impurity, the influence of crystal boundary to electrical property in the 5M BaIrO$_3$ is larger

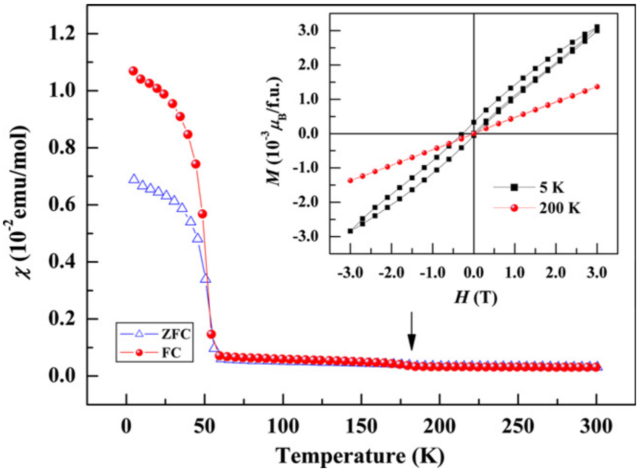

Fig. 3. Temperature dependences of magnetic susceptibility of the 5M $BaIrO_3$. The inset shows the M–H curves at different temperatures.

than that in the 6M $BaIrO_3$, which gives rise to worse metallicity of the 5M form.

The wave function of the 5d orbitals is highly extended, so the oxide iridates should be metallic. However, although the short Ir–Ir distance in the Ir_3O_{12} trioctahedron is propitious to metallic behavior, the 9M $BaIrO_3$ is not a metal at low temperature [11,13]. The strong antiferromagnetic exchange interaction between the adjacent Ir cations binds the activity of electrons, like that in the 9R $BaRuO_3$. Cao et al. thought that the twisting and distortion of the Ir_3O_{12} trioctahedron reduce the bandwidth, and give rise to the non-metallic behavior [11]. In the 5M $BaIrO_3$, two Ir_2O_9 dioctahedrons connect each other through the O ions in the corner, and then the two dioctahedrons and one IrO_6 octahedron arrange alternately along the c-axis. The binding of Ir–Ir exchange interaction to the electrons in the Ir_2O_9 dioctahedron is weaker than that in the Ir_3O_{12} trioctahedron of the 9M $BaIrO_3$, and the degree of twisting and distortion of the former is less than that of the latter, according to the XRD patterns [9]. For the small distortion in crystal structure and high extendability of orbital wave function, the 5M $BaIrO_3$ behaves with a metallic property, like the 6M $BaIrO_3$ [7].

Fig. 3 shows the temperature dependences of magnetic susceptibility of the 5M $BaIrO_3$ in the range of 5–300 K. The 5M $BaIrO_3$ is weak ferromagnetic, with the T_c 54.3 K. There is another transition from ferromagnetism to paramagnetism at about 183 K, indicated with an arrow in Fig. 3, which is attributed to the 9M form impurity in the 5M $BaIrO_3$. The M–H curves at 5 and 200 K are shown in the inset of Fig. 3. The hysteresis loop at 5 K indicates the weak ferromagnetism, and the small values of magnetic moment are consistent with the small susceptibility. The straight M–H relationship at 200 K indicates that the sample completely transfers to a paramagnet, although the 5M $BaIrO_3$ has already become a paramagnet above 55 K. Sr_2IrO_4 and $Sr_3Ir_2O_7$, which adopt the distorted Ruddlesden–Popper structure [19,20], are also weak ferromagnets, with T_c values of about 240 and 285 K, respectively [21,22]. But they are not metals [21,22], like the 9M $BaIrO_3$. Our present work adds one new metallic iridate of the 5M $BaIrO_3$ with weak ferromagnetism.

For the 5M $BaIrO_3$, the χ data in the paramagnetic regions can be fitted to the following equation:

$$\chi = \frac{C}{T-\theta} + \chi_0(1 - AT^2), \tag{1}$$

where the parameter C, θ, and χ_0 are the Curie constant, paramagnetic Curie temperature, and the temperature independent susceptibility, respectively. $A = (\pi^2 k_B^2/6)\{[N'(E_F)/N(E_F)]^2 - [N''(E_F)/N(E_F)]\}$, where $N(E_F)$ is the density of states at Fermi level (E_F) per atom, $N'(E_F)$ and $N''(E_F)$ are its first and second energy derivatives [23]. The effect magnetic moment μ_{eff} per Ir atom is equal to $0.215(7)\mu_B$, as obtained from C through the formula $\mu_{\mathrm{eff}} = 2.83\sqrt{C}$. The μ_{eff} is less than the theoretic spin-only value of about $1.73\mu_B$ for the $t_{2g}^5 e_g^0$ electronic state of Ir^{4+} cation with one unpaired 5d electron. The small Ir moments are also found for the Ir^{4+} cation in the 9M $BaIrO_3$ ($0.13\mu_B$/Ir) [11], the 6M $BaIrO_3$ ($0.276\ \mu_B$/Ir) [7], the perovskite $SrIrO_3$ ($0.117\mu_B$/Ir) [24], Sr_2IrO_4 ($0.50\mu_B$/Ir) [21], and $Sr_3Ir_2O_7$ ($0.69\mu_B$/Ir) [22]. The small value of μ_{eff} indicates that the Ir^{4+} cation partly loses the local moment, which is attributed to the strong spin–orbit coupling in Ir cations and the strong exchange interactions that lower the magnetization of the sample between adjacent Ir cations in the polyoctahedrons. The fitting χ_0 and A are equal to $2.98(2) \times 10^{-4}$ emu/mol and $3.6(2) \times 10^{-7}\,K^{-2}$, respectively. The μ_{eff} of the 6M $BaIrO_3$ is larger than that of the 5M form, because the proportion of IrO_6 octahedron in the former is larger than that in the latter [7]. For the 5M form, the paramagnetic Curie temperature θ of 51(5) K is positive, which is consistent with the weak ferromagnetism. So the weak ferromagnetism below 54.3 K is the intrinsic property of the 5M $BaIrO_3$.

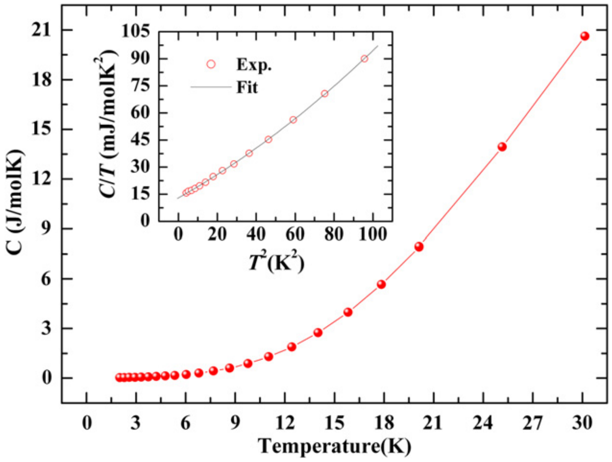

Fig. 4. Low-temperature specific heat of the 5M $BaIrO_3$. The inset shows the relationship of C/T versus T^2.

Up to now, there have been two different interpretations of the weak ferromagnetism in the 9M $BaIrO_3$. In Refs. [1,10], the authors thought that the spin canting between the two neighboring Ir_3O_{12} trioctahedrons gives rise to weak ferromagnetism. However, according to the data of a single crystal, Cao et al. thought the 9M $BaIrO_3$ is a true ferromagnetic material and its weak ferromagnetism originates from spin polarization rather than from spin canting [11]. In the 5M $BaIrO_3$, the arrangement of Ir–Ir dimmer is parallel in terms of the structural data [9]. The coupling of two Ir cations is also antiferromagnetic in one Ir_2O_9 dioctahedron, with the resultant spin of $S = 0$. According to the interpretation of spin canting, the 5M $BaIrO_3$ should be antiferromagnetic or paramagnetic, being contrary to the present experimental results. So the weak ferromagnetism of the 5M $BaIrO_3$ originates from spin polarization.

In order to investigate more about the physical property of the 5M $BaIrO_3$, we measured the low-temperature specific heat, with the C–T curve in the range of 2–30 K being shown in Fig. 4. The specific heat below 10 K can be fitted to the following equation:

$$C/T = \gamma + \beta T^2 + \delta T^4, \tag{2}$$

where the first term is the electronic contribution, the second term is the phonon contribution according to the Debye approximation, and the third term is the deviation from the linear dispersion of the acoustic modes in the extended temperature range. The relationship of C/T versus T^2 is shown in the inset of Fig. 4. The Debye temperature Θ_D is equal to 253(1) K, as obtained from β through the formula $\Theta_D = (1.944 \times 10^6 p/\beta)^{1/3}$, where the atom number per chemical formula unit (p) is equal to 5 for $BaIrO_3$. The Sommerfeld constant γ of 13.0(2) mJ/mol K^2 is obtained. The γ of the 5M $BaIrO_3$ is larger than that of the 6M form [7], which indicates that the metallicity of the former is better than that of the latter, because the proportion of direct Ir–Ir interaction in the former is larger than that in the latter.

The Wilson ratio R_W of the 5M $BaIrO_3$ is 1.67(4), as obtained from χ_0 and γ through the formula $R_W = 1/3(\pi k_B/\mu_B)^2(\chi_0/\gamma)$ [25]. The large Wilson ratio R_W indicates the enhancement of electron–electron correlation, although the temperature independent magnetic susceptibility χ_0 is in the range of the free electron system. The theoretic $N(E_F)$ of the 5M $BaIrO_3$ may be comparable to that of the 9M form, for the same chemical composition and similar structure. We used the $N(E_F)$ of about 4.0 state/(eV · f.u.) as the theoretic value [26], since no energy band structure calculation of the 5M $BaIrO_3$ has been performed. The theoretic Sommerfeld constant $\gamma^{\mathrm{th}} = 9.4$ mJ/(mol · K^2), as calculated from $N(E_F)$ through the formula $\gamma^{th} = \pi^2 k_B^2 N(E_F)/3$. The ratio of $m^*/m_0 (= \gamma/\gamma^{th})$ is equal to 1.38 for the 5M form, so the Pauli paramagnetic susceptibility χ_p is equal to $1.21\chi_0$, as obtained through the formula $\chi_0 = \chi_p + \chi_{di} = \chi_p[1 - 1/3(m_0/m^*)^2]$, where χ_{di} is the Landau diamagnetic susceptibility. According to this $N(E_F)$, the theoretic Pauli paramagnetic susceptibility χ_p^{th} is 1.29×10^{-4} emu/mol, as calculated from $N(E_F)$ through the formula $\chi_p^{th}=\mu_B^2 N(E_F)$, which is less than the experimental value. The Stoner enhancement factor S is 2.8, as obtained from χ_p and χ_p^{th} through the formula $S = \chi_p/\chi_p^{th} = [1 - IN(E_F)]^{-1}$, where I is the exchange integral that reflects the exchange splitting of energy band. The value of $IN(E_F)$ is equal to 0.64, which is in the range of electron–electron exchange enhancement, being consistent with R_W. According to the results of magnetic susceptibility and specific heat, there is a modest electron–electron correlation in the 5M $BaIrO_3$.

4. Conclusions

In summary, the 5M $BaIrO_3$ was synthesized by using the high-pressure and high-temperature method, and electrical resistivity, magnetic susceptibility, and specific heat were obtained.The 5M $BaIrO_3$ is intervenient in the 9M and 6M forms in the structure and physical properties. The measurements of electrical and magnetic properties showed that the 5M $BaIrO_3$ is a Fermi-Liquid metal with weak ferromagnetism. Specific heat data indicate the modest electron–electron correlation in the 5M $BaIrO_3$.

Acknowledgments

We thank Prof. C. Dong and H. Chen of Institute of Physics, Chinese Academy of Sciences for their help in XRD measurement and analysis, and the support from NSF and Ministry of Science and Technology of China through the research projects.

References

[1] R. Lindsay, W. Strange, B.L. Chamberland, R.O. Moyer Jr., Solid State Commun. 86 (1992) 759.
[2] P.C. Donohue, L. Katz, R. Ward, Inorg. Chem. 5 (1966) 335.
[3] P.C. Donohue, L. Katz, R. Ward, Inorg. Chem. 4 (1965) 306.
[4] J.M. Longo, J.A. Kafalas, Mater. Res. Bull. 3 (1968) 687.
[5] J.G. Zhao, L.X. Yang, Y. Yu, F.Y. Li, R.C. Yu, Z. Fang, L.C. Chen, C.Q. Jin, J. Solid State Chem. 180 (2007) 2816.
[6] T. Siegrist, B.L. Chamberland, J. Less-Common Met. 170 (1991) 93.
[7] J.G. Zhao, L.X. Yang, Y. Yu, F.Y. Li, R.C. Yu, C.Q. Jin, Inorg. Chem. 48 (2009) 4290.
[8] J.M. Longo, J.A. Kafalas, R.J. Arnott, J. Solid State Chem. 3 (1971) 174.
[9] J.G. Cheng, J.A. Alonso, E. Suard, J.S. Zhou, J.B. Goodenough, J. Am. Chem. Soc. 131 (2009) 7461.
[10] A.V. Powell, P.D. Battle, J. Alloys Comp. 191 (1993) 313.
[11] G. Cao, J.E. Crow, R.P. Guertin, P.F. Henning, C.C. Homes, M. Strongin, D.N. Basov, E. Lochner, Solid State Commun. 113 (2000) 657.
[12] T. Nakano, I. Terasaki, Phys. Rev. B 73 (2006) 195106.
[13] N.S. Kini, A. Bentien, S. Ramakrishnan, C. Geibel, Physica B 359–361 (2005) 1264.
[14] J.G. Zhao, L.X. Yang, K. Mydeen, F.Y. Li, R.C. Yu, C.Q. Jin, Solid State Commun. 148 (2008) 361.
[15] W.D. Ryden, A.W. Lawson, C.C. Sartain, Phys. Rev. B 1 (1970) 1494.
[16] W.D. Ryden, A.W. Lawson, J. Chem. Phys. 52 (1970) 6058.
[17] C.Q. Jin, J.S. Zhou, J.B. Goodenough, Q.Q. Liu, J.G. Zhao, L.X. Yang, Y. Yu, R.C. Yu, T. Katsura, A. Shatskiy, E. Ito, Proc. Natl. Acad. Sci. USA 105 (2008) 7115.
[18] J.S. Zhou, K. Matsubayashi, Y. Uwatoko, C.Q. Jin, J.G. Cheng, J.B. Goodenough, Q.Q. Liu, T. Katsura, A. Shatskiy, E. Ito, Phys. Rev. Lett. 101 (2008) 077206.
[19] Q. Huang, J.L. Soubeyroux, O. Chmaissem, L.N. Sora, A. Santoro, R.J. Cava, J.J. Krajewski, W.F. Peck Jr., J. Solid State Chem. 112 (1994) 355.
[20] H. Matsuhata, I. Nagai, Y. Yoshida, S. Hara, S.-I. Ikeda, N. Shirakawa, J. Solid State Chem. 177 (2004) 3776.
[21] G. Cao, J. Bolivar, S. McCall, J.E. Crow, R.P. Guertin, Phys. Rev. B 57 (1998) R11039.
[22] G. Cao, Y. Xin, C.S. Alexander, J.E. Crow, P. Schlottmann, M.K. Crawford, R.L. Harlow, W. Marshall, Phys. Rev. B 66 (2002) 214412.
[23] S.N. Kaul, A. Semwal, H.-E. Schaefer, Phys. Rev. B 62 (2000) 13892.
[24] J.G. Zhao, L.X. Yang, Y. Yu, F.Y. Li, R.C. Yu, Z. Fang, L.C. Chen, C.Q. Jin, J. Appl. Phys. 103 (2008) 103706.
[25] K.G. Wilson, Rev. Modern Phys. 47 (1975) 773.
[26] K. Maiti, Phys. Rev. B 73 (2006) 115119.